THE SIMULATION OF CO- AND CROSS-POLAR CHARACTERS OF RAINFALL DROPLETS AND CHAFF

Edvin Aldrian[1]

Abstract

The error analyses and simulations of the co- and cross-polar characters of chaff and rainfall have been done. Error analyses include the ZDR distribution, numbers of scaterers, the orientation and shape dependence, the system DC bias, the channel gain imbalance and the quantification errors. There is no effect of number of scatterers on the noise. The orientation and shape dependence study indicates wider frequency distribution of ZDR from chaff is because of the chaff's needle shape. The orientation of chaff contributes insignificantly to noises The noises has been reduced considerably after eliminating system DC bias and gaining more channel balance. Further possible source of error is the quantification error in data analyses. LDR is more useful than ZDR when both chaff and rain are present. The result suggests a possibility of using chaff's LDR in tracing air movement.

Intisari

Analisa error dan simulasi sifat co- dan cross-polar dari chaff dan butir-butir hujan telah dilakukan. Analisa error termasuk penyebaran ZDR, jumlah chaff atau bidang pemantul (scatterers), orientasi dan bentuk dari chaff, factor kesalahan DC, keseimbangan kedua kanal pada radar dan factor kesalahan kuantitatif unit. Tidak ada sumbangan kesalahan dari jumlah scatterers pada noise. Penelitian orientasi dan bentuk menunjukkan lebarnya penyebaran ZDR pada chaff karena bentuknya. Orientasi dari chaff tidak menyumbang factor kesalahan yang berarti. Noise telah dapat dikurangi hingga minimal setelah menghilangkan factor kesalahan system DC dan menyeimbangkan kedua kanal. Faktor kesalahan lainnya yang mungkin adalah kesalahan kuantitatif unit pada analisis data. LDR lebih berguna dari ZDR ketika kedua duanya yaitu chaff dan butir hujan berada. Hasil tersebut menyarankan kegunaan chaff LDR untuk pemantauan pergerakan udara.

Keyword: chaff, rain, error analyses, LDR, ZDR, co- and cross polarizations

1. INTRODUCTION

This study is an extension of a previous study by Aldrian (2002), to explore more on the co and cross-polar characteristics of chaff and rain droplets. In doing so we are utilizing a filter technique developed during that study to explore how those characters contribute to noise and error signals.

Due to shape and orientation differences, chaff and rain droplets shall have different noise characteristics and different probability distribution functions. Furthermore, there is a need to explore how can we reduce the error signals provided that we understand their characteristics. Since the CAMPR radar (Kumagai *et al.*, 1996) used in this study is limited to linearized polarized signals, only the linear characters of signals will be explored. CAMPR was developed by the Communications Research Laboratory (CRL), Japan. CAMPR uses a frequency of 13.8 GHz, which is nearly the same frequency as the precipitation radar installed in the TRMM satellite Simpson *et al.* (1998). One of the main purposes of CAMPR is to calibrate the TRMM Precipitation Radar (TRMM-PR) data. CAMPR has dual polarization and dual doppler

1. Max Planck Institut für Meteorologie, Hamburg, Germany

capabilities.

We will explore both chaff and rain droplet separately as well as together in a simulation. In this study, there were no experiments conducting together where chaff was distributed during rainy period. This can be achieved by making a simulated situation where chaff was released during rainfall period.

The outline of this paper is as follow. Section 2 discusses the data and some basic radar theories, section 3 some methods and simulation studies with regards to the error reduction. Section 4 discusses the chaff and rain coexistence simulation followed by section 5, which discusses the overall results. Finally, section 6 summarizes the conclusions.

2. DATA AND THEORY

The data was taken from the chaff and rain experiments conducted from November 29 until December 1, 1995 over the Japan Sea. The purpose of these experiments was to study the co-polar and the cross-polar radar reflectivity of chaff and rain. On November 29, we performed chaff measurements, while on the other days we performed rain measurements. During the chaff measurement, we varied elevation angles of the CAMPR antenna from nadir to near horizon. At this time we used two aircrafts: one scattered chaff, and the other carried CAMPR.

The chaff used in this experiment is thin conducting metal stripes whose width and thickness are very small compare to the radar wavelength, i.e. $L/d >> 1$ and $kd << 1$, where L is the length of the chaff, d is the width, and k is the wave number of the radar radio wave. The chaff used in this experiment has dimensions: L = 32 mm and d = 0.25 mm. Chaff was released from the first aircraft intermittently, while the second aircraft tracked chaff locations by scanning the CAMPR antenna. CAMPR has a simultaneous measurement capability for two orthogonal polarizations by using two receivers. There are 128 pairs of cross-polar (different polarization in transmitter and receiver) and co-polar (equal polarization on both transmitter and receiver) data.

During data processing we developed a filter method named the spectrum threshold filter to discriminate echoes of rain and chaff as well as noises (Aldrian, 2002). This filter method is applied throughout this study. According to Doviak and Zrnick (1993), in typical weather radar, the mean power $\overline{P}(\tau)$ over N_s number of hits is given by

$$\overline{P}(\tau) = \frac{1}{N_s}\sum_{i}^{N_s}\left|I_i^2 + Q_i^2\right| \quad (1)$$

The mean power intensity $\overline{P}$ is related to the radar reflectivity factor (Z) and a distance r according to a formula:

$$\overline{P}(r) = c\,\frac{Z}{r^2} \quad (2)$$

where c is a constant determined from the radar system parameters, and r is the distance from the radar to a hydrometeor. Since we use only relative values we hereafter neglect c.

There are four definitions of reflectivity according to their polarizations used in this work. If a signal is transmitted horizontally polarized and received vertically polarized, it is symbolized with Z_{hv}. In a similar fashion other reflectivity parameters used here are Z_{hh}, Z_{vv} and Z_{vh}. From these, two more radar observable parameters, which are used in this paper, are the *ZDR* (Differential Reflectivity) and the *LDR* (Linear Depolarization Ratio) which are defined as

$$ZDR = 10\log\left(\frac{Z_{hh}}{Z_{vv}}\right) \quad (3)$$

$$LDR = 10\log\left(\frac{Z_{vh}}{Z_{hh}}\right) \cong 10\log\left(\frac{Z_{hv}}{Z_{vv}}\right) \quad (4)$$

In this work the first (left) *LDR* definition is used.

3. METHODS

We made simulation studies in order to examine the co- and cross-polar characteristics of chaff and rain. At this time CAMPR has only the linear polarization. Thus main polarization characters available are *ZDR* and *LDR*. The simulation study on the *ZDR* will be discussed in the subsection *ZDR* distribution and the simulation study on the *LDR* will be discuss in the subsection rain and chaff coexistence.

3.1. The ZDR Distribution

The *ZDR* distribution is one of the indicators of the system polarization behavior. Since the *LDR* distribution does not apply quite well for the rain case due to a weak cross-polarization data, only a ZDR distribution analysis is presented here. In a vertical pointing case such as our aircraft observation, the mean of rain *ZDR* echoes in the frequency distribution diagram is expected at zero, the deviation shown here is due to the horizontal and the vertical channel mis-calibration or other causes. In this section we will examine some possible causes of this.

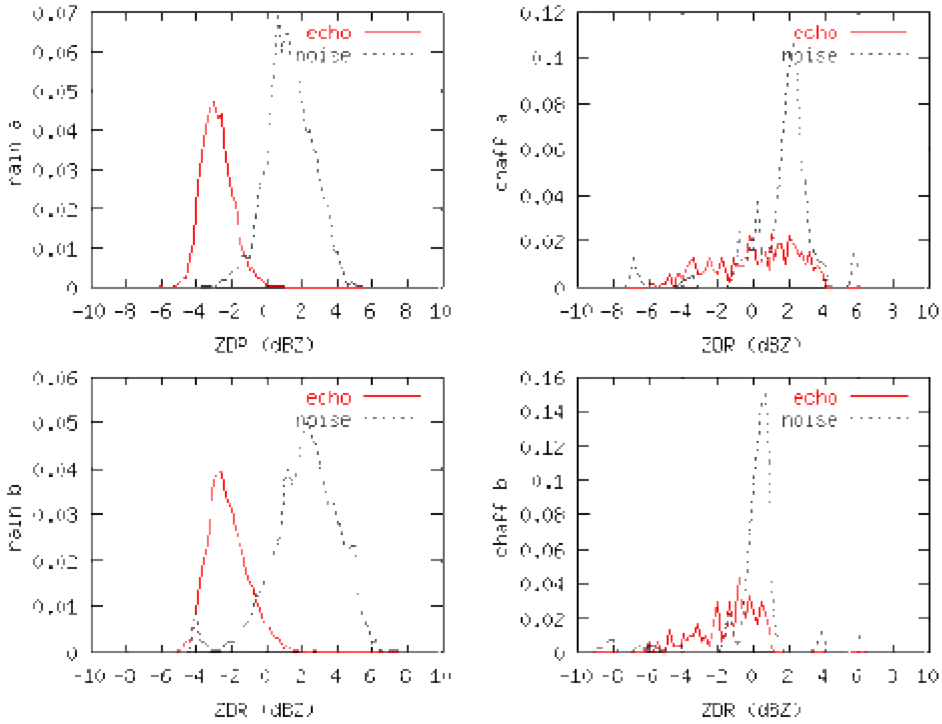

Figure 1. The *ZDR* frequency distribution of chaff and rain against their noise distribution

3.2. The Number of Scatterers

The frequency distribution diagrams of the *ZDR* (Fig. 1) show that chaff has random distributions, while rain has a Rayleigh type distribution. Note that *ZDR* is shown in a logarithmic scale. These facts maybe because raindrops have a near sphere shape but chaff have a needle shape. Hence the *ZDR* of chaff distributes much wider than that of the rain. Some people may think that this phenomenon is due to the number of scatterers. In fact number of scatterers of chaff is much less than that of rain. To understand the effect of numbers of scatterers in the power distribution, we performed a simulation study. In this study we prepare a set of random data of I (real) and Q (imaginary) components. This set makes up one radar echo. In calculating the average pulse power we use a similar number of hits as our chaff observation i.e. 256. Following Eq. 1, in which

$$I_i = \frac{\alpha}{S_{cat}} \sum_{n=1}^{S_{cat}} r \cdot \cos\theta_n \qquad (5)$$

$$Q_i = \frac{\alpha}{S_{cat}} \sum_{n=1}^{S_{cat}} r \cdot \sin\theta_n \qquad (6)$$

Here N_s equals 256, S_{cat} is a variable determining the number of scatterers, α is a constant determined by radar parameters, and θ is a uniform random number between 0 and 2π. Angle θ represents the back scatterer phase difference. This simulation result in Fig. 2 shows no significant effects of the number of scatterers to the power distribution.

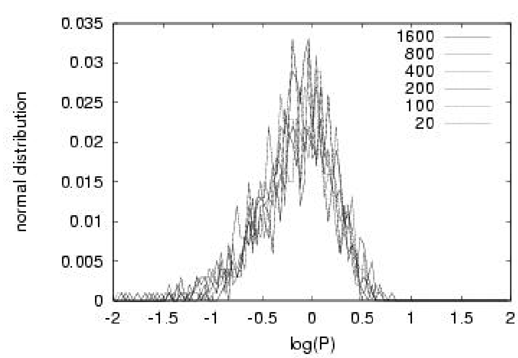

Figure 2. Simulations of number of scatterer against power distribution for number of scatterers from 20 to 1600. All curves are normal distribution of 500 points sample.

3.3. The Orientation and the Shape Dependence

We also did a simulation study on the orientation dependence of the *ZDR* distribution. According to Van de Hulst (1957), when an incident wave, $\overrightarrow{E_0}$ is parallel to one of the principle axes of an ellipsoid scatterer, the electric field $\overrightarrow{E}$ at any point inside the ellipsoid is given by

$$\vec{E} = \overrightarrow{E_0} - L_i 4\pi \vec{P} \qquad (7)$$

where L_i are the three factors depending on the ratios of the axes and $\vec{P}$ is a polarization vector. The dipole moment, $\vec{p}$ of a solid particle in an electric field is

$$\vec{p} = \int \vec{P} dV \qquad (8)$$

where the polarization vector is given by

$$\vec{P} = (m^2 - 1)(\vec{E} / 4\pi) \qquad (9)$$

where *m* is a complex refractive index. For a homogeneous material we have a dipole moment given as

$$\vec{p} = \vec{P}V = \alpha \overrightarrow{E_0} \qquad (10)$$

where α is a 3 x 3 matrix.

Then using an orthogonal coordinate with axes parallel to the principal axes of the ellipsoid, the dipole moment, Eq. 10 can be written as

$$\vec{p} = \begin{pmatrix} \alpha_1 & 0 & 0 \\ 0 & \alpha_2 & 0 \\ 0 & 0 & \alpha_3 \end{pmatrix} \begin{pmatrix} E_{01} \\ E_{02} \\ E_{03} \end{pmatrix} \qquad (11)$$

where α_i is given by

$$\frac{V}{4\pi\alpha_i} = L_i + \frac{1}{m^2 - 1} \qquad (12)$$

In the metallic or the chaff case, $m^2 >> 1$, thus the second term on the right hand side of Eq. 12 can be neglected. For any arbitrary ratio of semi axes *a*, *b* and *c* we have

$$L_1 = \int_0^\infty \frac{abc \quad ds}{2(s+a^2)^{3/2}(s+b^2)^{1/2}(s+c^2)^{1/2}} \qquad (13)$$

and the same is applied for L_2 and L_3 where the relation

$$L_1 + L_2 + L_3 = 1 \qquad (14)$$

holds. These *L*'s characterize chaff as needle shape (elongated ellipsoidal) scatterers and raindrops as near sphere shape (oblate spheroid) scatterers (Table 1). Figure 3 illustrates coordinate axes used in this simulation. As shown in Fig. 3, the simulation is determined by the choices of θ_1

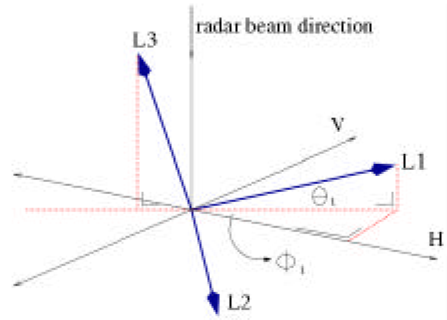

Figure 3. Coordinate axes of incoming beam, H or V polarization, L1, L2 and L3 directions.

Table 1. Chaff and rain dimensions (Battan, 1973)

	Rain	Chaff
A	1	128
B	1	1
C	0.8	9.001
L_1	0.30278	3.19128×10^{-6}
L_2	0.39444	0.0098995
L_3	0.30278	0.9900098
m (λ=3.21cm,0^{0}C)	7.14+2.89i	$m^2 >> 1$
m (λ=3.21cm,0^{0}C)	7.8+2.44i	$m^2 >> 1$

and ϕ_1.

Since the dipole moment square, $|\vec{p}|^2$ is linearly proportional to the power intensity, $\overline{P}$ (Eq. 1}) then *ZDR* can be calculated using the following ratio:

$$ZDR \equiv \frac{\sum_n \left|\sum_i e^{j\theta i} \alpha \vec{E}_{horiz}\right|^2}{\sum_n \left|\sum_i e^{j\theta i} \alpha \vec{E}_{vert}\right|^2} \qquad (15)$$

where α has components α_1, α_2, α_3 and the factor $\sum_i e^{j\theta i}$ accounts for the overall chaff population in the radar scanning volume, which is randomly scattered by a phase difference θ_i. In this simulation the chaff dimension as described in Section 2 was used and for rain we used the oblate spheroid shape

The result of this simulation shows that the variation in ϕ_1 affects the result significantly, which indicates a horizontal orientation dependence on the chaff *ZDR* values. The result in Fig. 4 has random ϕ_1 and θ_i values. Like before the result gives no clue of the dependence of the number of scatterers over a sampling volume. For a quantitative comparison we fit the result with a Gaussian distribution by using the Simplex method

(Press, *et al*., 1996) to compare simulation results of chaff and rain with their corresponding observed data using some gaussian parameters, i.e. the amplitude (A_{mp}), the central peak (α) and the gaussian width (σ). These parameters are defined as follows

$$y = A_{mp} e^{-(x-a)^2/s^2} \qquad (16)$$

The choice of the gaussian shape is a hypothetical assumption only and we though it would fit well. Because we have an exact number of data, the A_{mp} and σ parameters depend on each other. The larger A_{mp} is, the smaller σ is. σ indicates the distribution width. Usually the following relation holds

$$s_e^2 = s_b^2 + s_s^2 \qquad (17)$$

where σ_e, σ_b and σ_s are the echo, the background and the system error, respectively. The summary of these comparative results is shown in Table 2. The table shows narrower raindrops distributions than chaff ones. Thus the peak amplitude (A_{mp}) of chaff is lower than that of raindrop. The simulation results have much narrower distribution than the observed data. However, the simulation qualitatively agrees well with observation, i.e. the rain distribution has a gaussian type distribution and the chaff distribution has a fluctuating shape. This simulation suggests that the fluctuating of the *ZDR* distribution is not because of the preferable chaff orientation but due to the needle shape. The width and center of the distribution is also affected by system errors. Under an ideal condition, background noises should yield *ZDR* values at around zero, since their signals are receiver noise. This fact is our reference in the system error correction process. There are possible contributions of errors other than the background noise. These possible errors are the DC bias, the channel gain imbalance and the quantification errors.

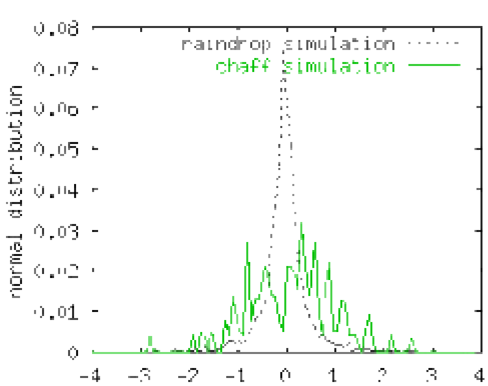

Figure 4. A simulation of orientation dependence of *ZDR* vs normal distribution. The curves shows *ZDR* distribution with θ_1 and ϕ_1 random angle from 0 to 2π. Dashed line is rain distribution, solid line is chaff.

Table 2 Chaff and rain *ZDR* distributions with Gaussian parameters

		A_{mp}	α	σ
Chaff	case A	0.01596	0.5624	3.5925
	case B	0.02809	-0.7829	1.8215
	simulation	0.0178	0.0254	1.2497
Rain	case A	0.0474	-2.9394	1.1733
	case B	0.0370	-2.4319	1.4888
	simulation	0.06067	-0.0488	0.3138

3.4. The System DC Bias

This error is not caused by an external factor but rather mainly by the performance of the system itself. Subtracting individual signal by its average can reduce this error. One way to do this is by modifying Eq. 1 as follows

$$\overline{P}(t) = \frac{1}{N_s}\sum_{i}^{N_s}\left|\left(I_i - \overline{I}\right)^2 + \left(Q_i - \overline{Q}\right)^2\right| \qquad (18)$$

where $\overline{I}$ and $\overline{Q}$ are average values over specified contiguous hits. This type of error exists on each channel and is independent of the other two types of errors. Figure 5 illustrates the result after applying Eq. 18 to Fig. 1.

As the result of this modification, background noises are suppressed by 10 – 15 dB, centered around 0 dB and have a narrower distribution than before. These results indicate the existence of a DC bias error in the system. One disadvantage of this scheme is that $\overline{I}$ and $\overline{Q}$ are localized constants of one specified contiguous hit and is not exactly the true DC bias, which should be constant throughout all the data. Thus, we have some variation of suppressed value from 10 - 15 dB. For one system this value should be a constant regardless of the time of observation. The second problem is that the DC bias has range gate dependence. The biases at gates near CAMPR have higher values than those of far end range gates. The third problem is that the DC bias in one set of a contiguous hit is not always constant, i.e. there could exist more than one localized DC biases. We could not easily obtain the true DC bias error of the system but this scheme is enough to reduce the effect.

3.5. The Channel Gain Imbalance

This type of error is also due to the system. CAMPR has two receiver channels (the horizontal

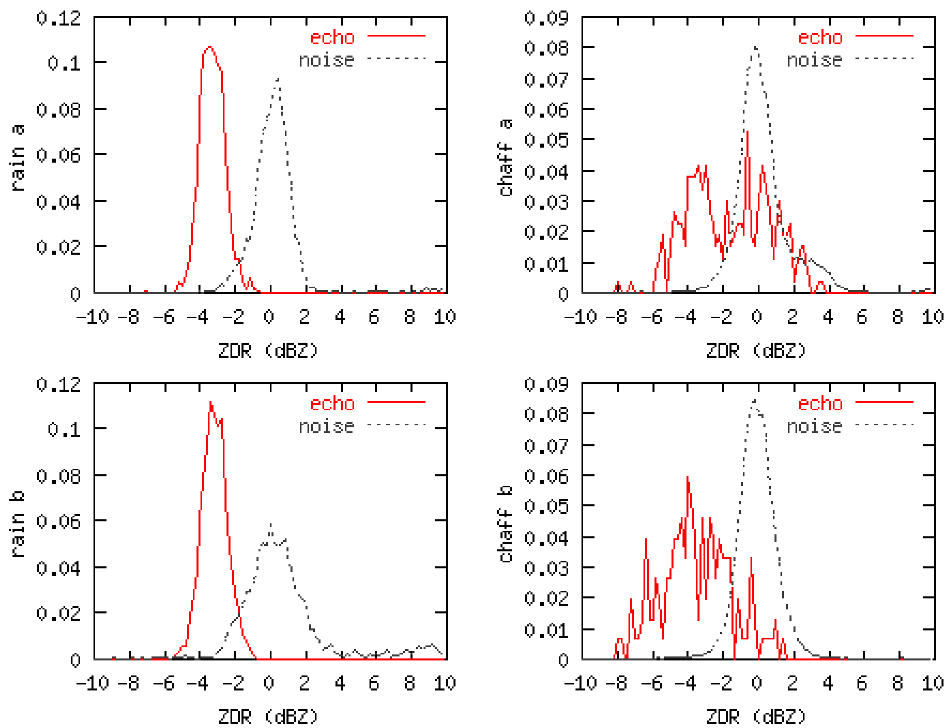

Figure 5. A modification of Fig. 1 after removing DC biases.

and the vertical polarization channels), which are independent to each other. The calibration of these channels has a great effect on the CAMPR overall data analysis. One major indication of this is the error from the *ZDR* distribution. Since *ZDR* represents both co-polarization signals of those channels we expect that noises would have values centered around zero. As the result this did not happen, which is a major indication of the existence of this noise. We could not know exactly how much this error is, but we can eliminate this by subtracting the cross-polar power (dB) from the co-polar power (dB) under an assumption that this error always exists in both channels. As discussed before, rain has a much weaker cross-polarization data than the co-polar one, but chaff has a much strong cross-polar data than the co-polar one. Thus, according to this scheme, we would expect that this noise reduction scheme work for chaff better than for rain. As a summary, this noise correction is applied by modifying the ZDR equation (Eq. 3) as

$$ZDR = 10\log\left(\frac{Z_{hh}}{Z_{vv}}\right) - 10\log\left(\frac{Z_{vh}}{Z_{hv}}\right) \quad (19)$$

After applying this scheme, the noise of chaff and rain will be centered around zero as the major indication of the existence of this noise. The direct result of this scheme is not shown here. Figure 6 shows the result using the system DC bias and the gain correction. Again all noises are centered around zero but they still have a wide distribution as before. On the other hand, the echo distributions have improved significantly compared to the original (Fig. 1) as shown by a narrower distribution and a higher peak. Chaff echo distributions are also improved as they became more like a gaussian type. Qualitatively all chaff and rain echo distributions agree well with the simulation result in Fig. 4. One weak point is that noise distributions are not exactly centered on zero. One possible explanation is the difference in receiver noises in both channels. The other weak point is that noises still have wider distributions than echo, which is unexpected since the echo distribution width or σ^2 should be summation of all σ^2 from the background noise, the system, and the echo itself. Possible explanation of this is the quantification error.

3.6. *The Quantification Errors*

The basic idea is that the quantification error exists in *ZDR* calculation because *ZDR* is the difference in a logarithmic average of a fluctuating dataset. Low average values have more quantification errors than higher average values. As a result, the background noise has a higher probability of a wider distribution σ^2 than echo. From observation data of chaff, the noise signal level is around ±3 units and the echo signal is fluctuating ±50 units. We have an absolute

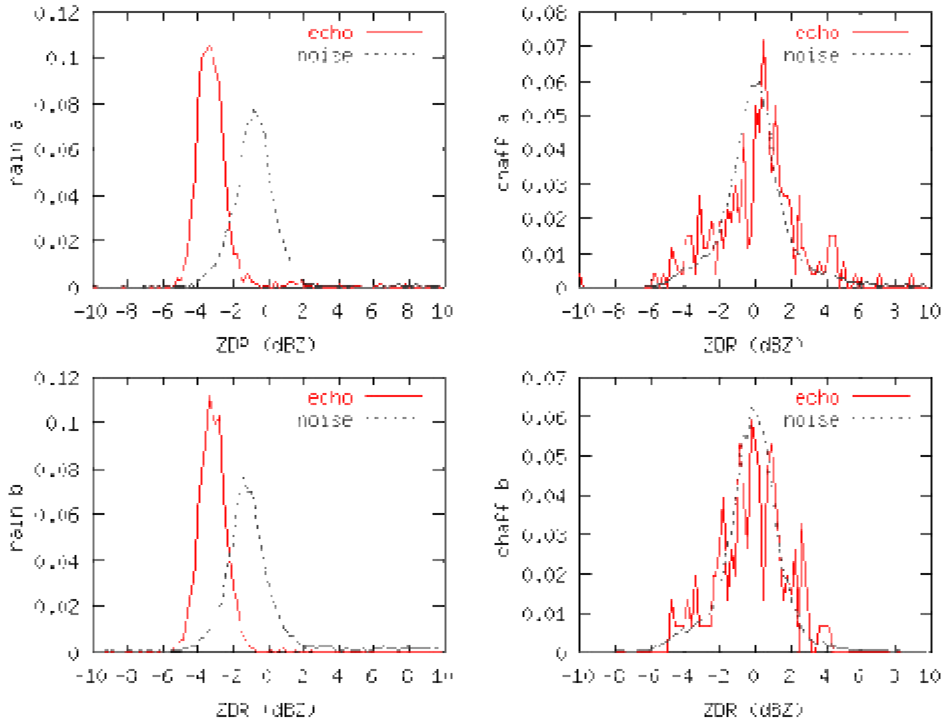

Figure 6. A modification of Fig. 1 after removing DC biases and gain imbalance. Com pare these echo distributions with the simulation result in Fig. 4

digitizing error 0.5 unit, i.e. noise has values of 3.0 ± 0.5 and echo 50 ± 0.5. If we include this error in the power calculation (Eq. 1) we have a contribution of this error to noise 0.125 x [10 log(3.5^2) - 10 log(2.5^2)] which equal to 0.1185 dB. Where in echo case we have 0.125 x [10 log(50.5^2) - 10 log(49.5^2)] which give error 0.0219 dB. The factor 0.125 in above calculations is from the averaging 128 hits and the summation of $\overline{I}$ and $\overline{Q}$. Relatively, the quantification error of the noise is much bigger than that of echo. However, Their absolute values are quite small or not significant.

4. THE CHAFF AND RAIN CO-EXISTANCE

In the beginning, the chaff experiment was aimed to show the CAMPR performance on known scatterer materials other than cloud hydrometeors. Thus at that time there was no plan to have an experiment of chaff presence in a rain situation. After the spectrum threshold filter technique was proved to be useful, we wanted to have data where both chaff and rain exist and to see the filter performance in that situation. In doing so, we made a simulation study using available data.

Table 3. Chaff and rain dataset specification

	Rain	Chaff
Antenna scan	0^o (fixed)	-20^o to 20^o (scan)
Range gate	100	40
Number of hits	512	256
Subsets	71	480
PRF*	2 kHz	4 kHz
Pulse width	0.5 µs	0.5µs
Sample rate	2 times	2 times
Sending mode	HV	HV

*PRF = Pulse Repetition Frequency

Table 4. Schematic hits adjustment. Only underline hits are used, rain hit from 129 to 512 are skipped

rain	H V H V H V H V H	...128
chaff	HVHVHVHVHVHVHVHVHV	...256
simulated	H V H V H V H V H	...128

This is done by combining both rain and chaff data into a new data set. The simulated data consist of the summation of chaff and rain signal per hits. Chaff and rain datasets differ in two main parameters as shown in Table 3. The first one is the number of hits and second one is PRF. In creating a simulated data we also need to take care of the polarization mode, which is similar in both cases i.e. HV (Horizontal-Vertical). As the result, the simulated data has a PRF of 2 kHz and a number of hits 128. Table 4 summarizes the combination method used in this simulation. In other words, this mechanism reduces the rain data by three fourths and reduces the chaff data by half. This data reduction does not cause any significant changes in the power intensity.

However, the rain data reduction causes the Nyquist folding (aliasing) problem. The original data has a frequency double than the simulated one. The doppler spectrum folding makes the spectral peak less sharp. This effect is sometimes significant for rain case but not for the chaff case, thanks to its sharp spectral peak.

Comparing to original rain data, the simulated data have some strong cross polarization signatures due to the chaff presence. In the real rain situation possible rain-chaff interaction needs a special attention. List *et al.* (1974) discussed the entrainment of chaff by rain, which was used to track the air motion. Figure 7 shows the simulated echo with rain and chaff. The chaff echoes appear at a height around 3.0 km. For the simulation, we added the chaff signal to rain only up to the range bin 40. Thus, we have the noise level difference farther than gate 40 (corresponding height is around 2.0 km). The chaff echo is sometimes indistinguishable from rain echo.

From the scatter diagram of the simulated data in Fig. 8, chaff ZDR signatures are totally embedded in the rain area, which shows that the ZDR is not effective to discriminate chaff from rain. On the other hand, from the chaff LDR diagram, chaff has a much higher LDR than rain. Even with these weak echoes the chaff LDR is separable from the rain LDR. Thus, the LDR signature is a good way to discriminate chaff from rain. Chaff LDR has values from above -5 dB up to around 5 dB while rain LDR has values below -5 dB.

5. DISCUSSIONS

The result presented here is in agreement with the work by Moninger and Kropfli (1987), where they concluded that the chaff *ZDR* technique is quite inferior to the *CDR* (Circular Depolarization Ratio). One reason is because the *ZDR* is sensitive to chaff orientation. At least for the vertical pointing case, chaff filaments are randomly oriented as the frequency distribution diagram (Fig. 1) also suggests. Only if chaff falling with a preferred orientation (as it does in still air) Z_{hh} and Z_{vv} differ greatly, which results in a significant *ZDR* value. However, we proved that the chaff needle shape causes that chaff distribution, not the preferred orientation. Moninger and Kropfli (1987) and later Reinking and Martner (1996) utilized the *CDR* technique in their studies. We did not do any *CDR* measurement, because at this time CAMPR was incapable of doing so. A complete general treatment of the linear polarization error in two channels system including the *LDR* and the *CDR* is given by McCormick (1981). His work did not distinguish the linear and the circular polarization clearly, but treated both as an equal case. In fact, the *LDR* and *CDR* have a very close physical meaning. *LDR* results in this work suggest a significant importance of using chaff as an air movement tracer.

Using our filter, the chaff *LDR* data should be used to detect the air movement as the chaff *CDR* used by Moninger and Kropfli (1987) and Reinking and Martner (1996). Guo and Uberall (1992) explained that in the chaff case no matter what the polarization of the transmitter radio waves, the

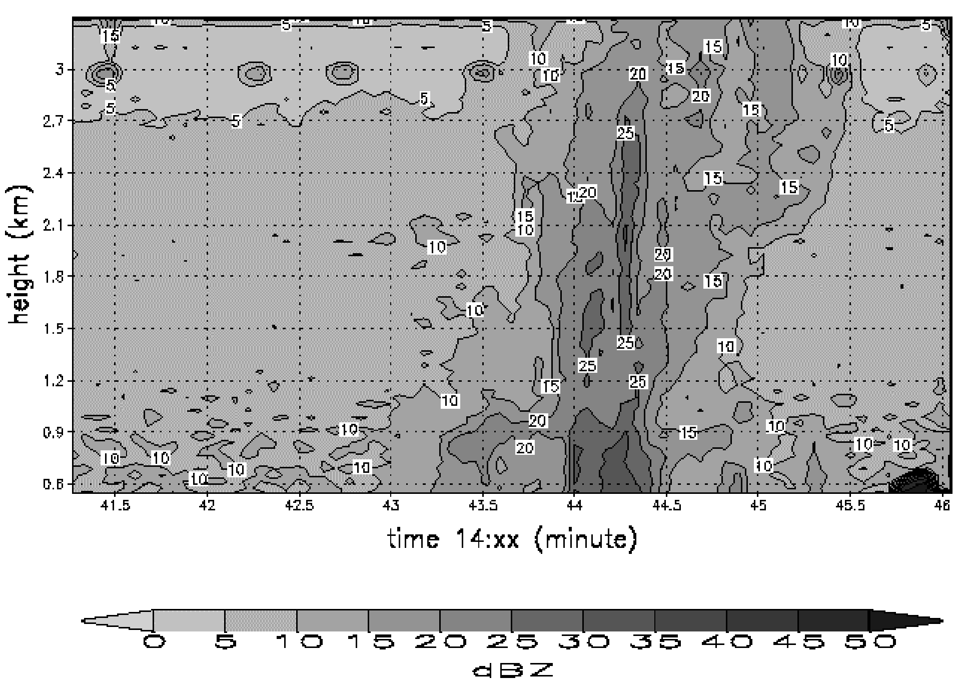

Figure 7. The simulated coexistence of data refrectivity after a DC bias elimination.

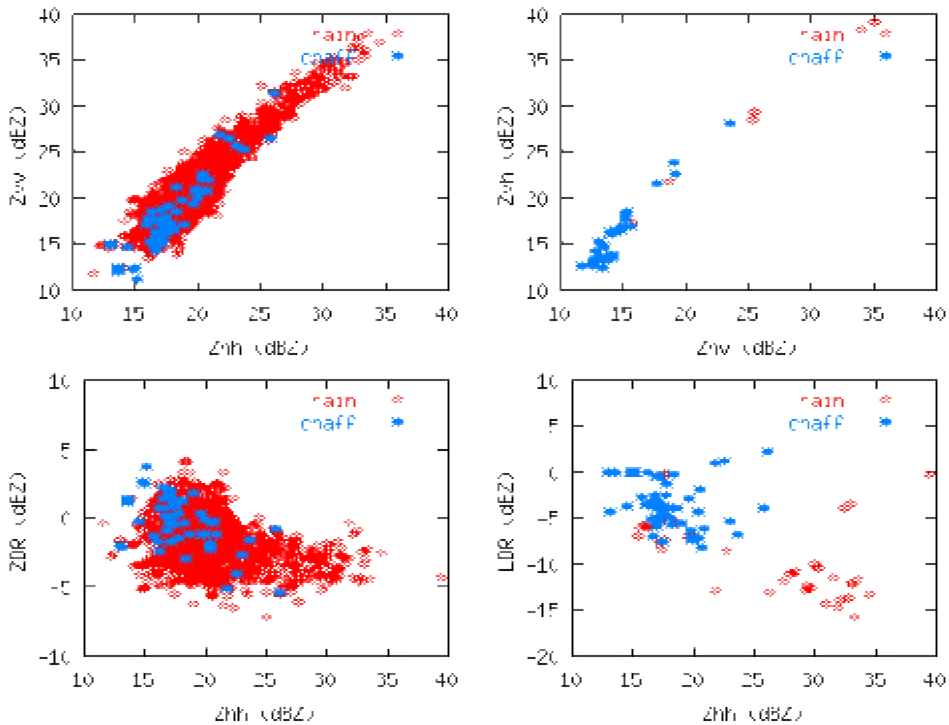

Figure 8. A filtered simulated data with range correction using A_{th} 0.6

scattered electric field vector is always linearly polarized. This leads to strong cross-polar chaff signatures so that chaff has meaningful *LDR* signatures. Consequently in an observation at a near nadir position, it is better to use the chaff's *LDR* than the chaff reflectivity alone especially in measuring the vertical velocity. Since chaff is a relatively light material and in the vertical movement rain has a higher velocity than chaff (1 m/s in still air), thus chaff is a good target for radar. Furthermore we also proved that chaff could be distinguished from rain by using the chaff's *LDR*, so that it is a good idea to use the chaff's *LDR* as a good air movement tracer. Lastly, the future in-situ research on the storm vertical structure with airborne radar is quite possible.

The Signal to Noise Ratio (SNR) diagram of chaff and rain (Fig. 9) shows that in most cases the rain SNR is higher than the chaff SNR. Although the experiment was conducted in a light rain period, the overall chaff SNR peaks are lower than the rain SNR peaks. From the SNR of the simulated data (Fig. 9), the region where only rain data exists (above gate 40), the simulated data show good agreement with the original dataset even though some data reductions already took place. Below gate 40 chaff signals affects the SNR diagram.

6. CONCLUSIONS

We have performed some error analyses of chaff and rain based on their co- and cross-polar properties. The error analyses include the ZDR distribution, numbers of scaterers, the orientation and shape dependence, the system DC bias, the channel gain imbalance and the quantification errors. We simulated the number of scatterers and the orientation and shape of hydrometeors. We have also done a simulated chaff presence in rainy condition.

In an air movement detection suggested here, chaff *LDR* is very effective. However, we need a polarization doppler radar to apply the *LDR* method and such a radar is much more expensive than the conventional one. Moreover, to pick up weak signatures we may need to apply this filter method, which requires a full doppler spectrum analysis. These are some drawbacks of the spectrum threshold filter method.

We also studied the frequency distribution of *ZDR* from rain and chaff. We found that chaff *ZDR* has wider distribution than rain. This is mainly due to the chaff's needle shape. In *ZDR* distribution analysis we found at least three significant sources of errors in the system, they are the DC bias, the gain imbalance and the quantification error. By correcting these errors we obtain a good agreement between *ZDR* frequency distribution from observations and the simulation.

We found that chaff *LDR* is higher than rain *LDR*. We conclude that chaff's *LDR* can be used as a good tracer of air movement observable from airborne radar. Chaff usage overcomes some limitations of using cloud hydrometeors as tracer, which has poor cross-polarization signature. This

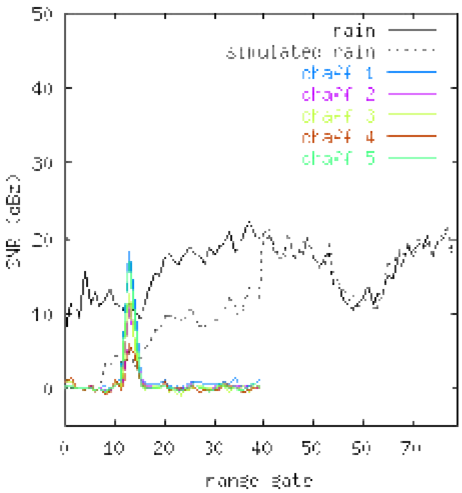

Figure 9. The SNR of rain, chaff and simulated data, chaff only has 40 gates while rain only shows the one above surface or up to gate 79. The rain data is taken at the extreme case, and chaff data are taken from various time set.

advantage is made possible with the use of the spectrum threshold filter method (Aldrian, 2002).

7. ACKNOWLEDGEMENT

This research was done in the Institute for Hydrospheric and Atmospheric Sciences, Nagoya University, Japan with funding from the Japanese Education minister (Monbusho). The author is very grateful to Prof. Kenji Nakamura as the supervisor, as well as I. Tamagawa, H. Minda, Y. Ohsaki and T. Iguchi who help me in developing the program and apparatus.

References

Aldrian, E., 2002: The spectrum threshold filter method for chaff and rain, *J. Sains & Tek. Mod. Cuaca*, **3**, 29-37

Battan, L. J., 1973: Radar observation of the atmosphere, Univ. of Chicago Press, Chicago, 17-40

Doviak, R. J. and D. S. Zrnic, 1993: *Doppler radar and weather observation*, Academic Press Inc., 562 pp

Guo, Y. and H. Uberall, 1992: Bistatic radar scattering by a chaff cloud, *IEEE Trans. Antenna Propagat.*, **40**, 837-841

Kumagai, H. et al., 1996: CRL Airborne Multiparameter Precipitation Radar (CAMPR): System description and preliminary results, *IEICE Trans. Commun.*, **E-79**-B, 770-776

List, R, T.B. Low and J.D. McTaggart-Cowan, 1974: Collision of Raindrop with chaff, *J. Appl. Meteor.*, **13**, 796-799

McCormick, G.C., 1981: Polarization errors in two-channel system, *Radio Science*, **16**, 67-75

Moninger, W. R. and R. A. Kropfli, 1987: A technique to measure entrainment in cloud by dual-polarization radar and chaff, *J. Atmos Ocean. Tech.*, **4**, 75-83

Press, W. H., S. A. Teukolsky, W. T. Vetterling, B. P. Flannery, 1996: Numerical Recipes in C, 2nd edition, Cambridge Univ. Press., 408-412, 994pp

Reinking, R. F. and B. E. Martner, 1996: Feeder-cell ingestion of seeding aerosol from cloud base determined by tracking radar chaff, *J. Appl. Meteor.*, **35**, 1402-1415

Simpson, J., R. F. Adler and G. R. North, 1998: A proposed tropical rainfall measuring mission (TRMM) satellite, *Bull. Amer. Meteor. Soc.*, **69**, 278-295

BIOGRAPHY

EDVIN ALDRIAN. Born in Jakarta, 2 August 1969, received Bachelor degree in Engineering Physics in McMaster University Canada, 1993, received Master of Science in Earth Science in Radar Meteorology from Nagoya University Japan, 1998. Now doing a Doctoral degree in Max Planck Institut für Meteorologie, Germany. Work as a scientist in UPT Hujan Buatan, BPPT since November 1993. Participating several short courses: STMDP preparation program, 1988-1989; short course on Meteorology in UI, March 1995; training on data analysis of wind profiler radar in Radio Atmospheric Science Center, Kyoto University, Japan, November 1995; basic training Geographic Information System, Geography Dept. UI, June 1996; International Hydrology Programme Training Course with topic Ice and Snow Hydrology, IHAS, Nagoya University and UNESCO, March 1998; Visiting scientist in Max Planck Institut für Meteorologie, Hamburg, learn the Indonesian climate variability and ECHAM GCM, Jan – March and July – September 1999; Advanced Course: Climate change in the mediterranean region part I: physical Aspects, The Abdus Salam International Center for Theoretical Physics ICTP, Trieste, Italy, March 2001; short course on Meteorology: Predictability, Diagnostics and Seasonal Forecasting, European Center for Medium Range Weather Forecast (ECMWF), Reading, UK, April 2001; PRISM/COACh Summer School on Climate Modelling, Max Planck Institut für Meteorologie-KNMI The Netherlands, Les Diablerets, Switzerland; School on the physics of the Equatorial Atmosphere, ICTP, Trieste, Italy, September 2001; Seminar on Predictability of Weather and Climate, ECMWF, Reading, UK, September 2002.